Detection and characterization of ticlopidine conjugates in rat bile using high-resolution mass spectrometry: applications of various data acquisition and processing tools

Fuying Du,[a] Qian Ruan,[b] Mingshe Zhu[b]* and Jie Xing[a]*

Ticlopidine, an antiplatelet drug, undergoes extensive oxidative metabolism to form *S*-oxide, *N*-oxide, hydroxylated and dealkylated metabolites. However, metabolism of ticlopidine via conjugation has not been thoroughly investigated. In this study, multiple data acquisition and processing tools were applied to the detection and characterization of ticlopidine conjugates in rat bile. Accurate full-scan mass spectrometry (MS) and collision-induced dissociation (CID) MS/MS data sets were recorded using isotope pattern-dependent acquisition on an LTQ/Orbitrap system. In addition, mass spectral data from online H/D exchanging and high collision energy dissociation (HCD) were recorded. Data processes were carried out using extracted ion chromatography (EIC), mass defect filter (MDF) and isotope pattern filter (IPF). The total ion chromatogram displayed a few major conjugated metabolites and many endogenous components. Profiles from EIC and IPF processes exhibited multiple conjugates with no or minimal false positives. However, ticlopidine conjugates that were not predictable or lost a chorine atom were not found by EIC or IPF, respectively. MDF was able to detect almost all of ticlopidine conjugates although it led to a few more false positives. In addition to CID spectra, data from HCD, H/D exchanging experiments and isotope pattern simulation facilitated structural characterization of unknown conjugates. Consequently, 20 significant ticlopidine conjugates, including glucuronide, glutathione, cysteinylglycine, cysteine and *N*-acetylcysteine conjugates, were identified in rat bile, a majority of which are associated with bioactivation and not previously reported. This study demonstrates the utility and limitation of various high-resolution MS-based data acquisition and processing techniques in detection and characterization of conjugated metabolites. Copyright © 2013 John Wiley & Sons, Ltd.

Supporting information may be found in the online version of this article.

Keywords: ticlopidine; conjugates; high-resolution mass spectrometry; mass defect filter; isotope pattern filter

Introduction

Ticlopidine is a noncompetitive adenosine diphosphate (ADP) receptor antagonist that inhibits platelet aggregation induced by ADP, and it has been widely used for the secondary prevention of atherothrombosis. Ticlopidine is also as effective as aspirin in preventing cardiovascular events in cerebrovascular, cardiovascular and peripheral vascular diseases.[1] However, ticlopidine can cause a series of adverse effects, including skin rashes, diarrhea, neutropenia and agranulocytosis.[2,3] The bioactivation of ticlopidine to reactive metabolites and their subsequent covalent binding to cellular macromolecules are thought to be involved in the occurrence of idiosyncratic hepatotoxicity in patients.[4]

Ticlopidine undergoes extensive metabolism in humans. About 60% of the dose is excreted into urine, where there is only a trace amount of the drug. The parent drug accounts for one-third of the radioactivity in the feces.[5] *In vitro* metabolism studies of ticlopidine in human liver microsomes (HLM) and rat liver S9 showed that major metabolic reactions are *N*-dealkylation, *N*-oxidation, the formation of dihydrothienopyridinium (M23), thienopyridinium (M24) (Fig. 1), thiophene *S*-oxidation and thiophene epoxidation.[6,7] Some of these oxidative metabolites were also found in rats and humans. Reactive intermediates from thiophene-epoxidation (M21), *S*-oxidation (M22) and epoxidation

of the chlorophenyl ring (M25) can be trapped by glutathione (GSH) *in vitro* and may lead to protein covalent bindings (Fig. 1).[4,8,9] In addition, the ticlopidine *S*-oxide intermediate can form a dimer *in vitro*.[10] A radiolabeled drug disposition study[7] found that a GSH adduct of ticlopidine *S*-oxide (M11) is a main biliary metabolite in rats although multiple major radioactive components remain to be identified.

Traditionally, triple quadrupole mass spectrometry (MS) is employed for detection and characterization of conjugated metabolites. In the experiments, constant neutral loss (NL)[11] and precursor ion (PI) scans[12] are carried out for screening conjugated metabolites based on unique fragmentations of various drug conjugates. For example, positive NL scan of 176 Da and negative PI scan of *m/z* 272 are routinely applied to the detection of glucuronide and GSH conjugates, respectively. However, to find different types of conjugates, multiple liquid

* Correspondence to: Jie Xing, School of Pharmaceutical Sciences, Shandong University, 44# West Wenhua Road, Jinan 250012, China. Email: xingjie@sdu.edu.cn

* Mingshe Zhu, Biotransformation Dept, Bristol-Myers Squibb, Princeton, NJ 08543, USA. E–mail: cMingshe.zhu@bms.com

a School of Pharmaceutical Sciences, Shandong University, Jinan, China

b Department of Biotransformation, Bristol-Myers Squibb, New Jersey, USA
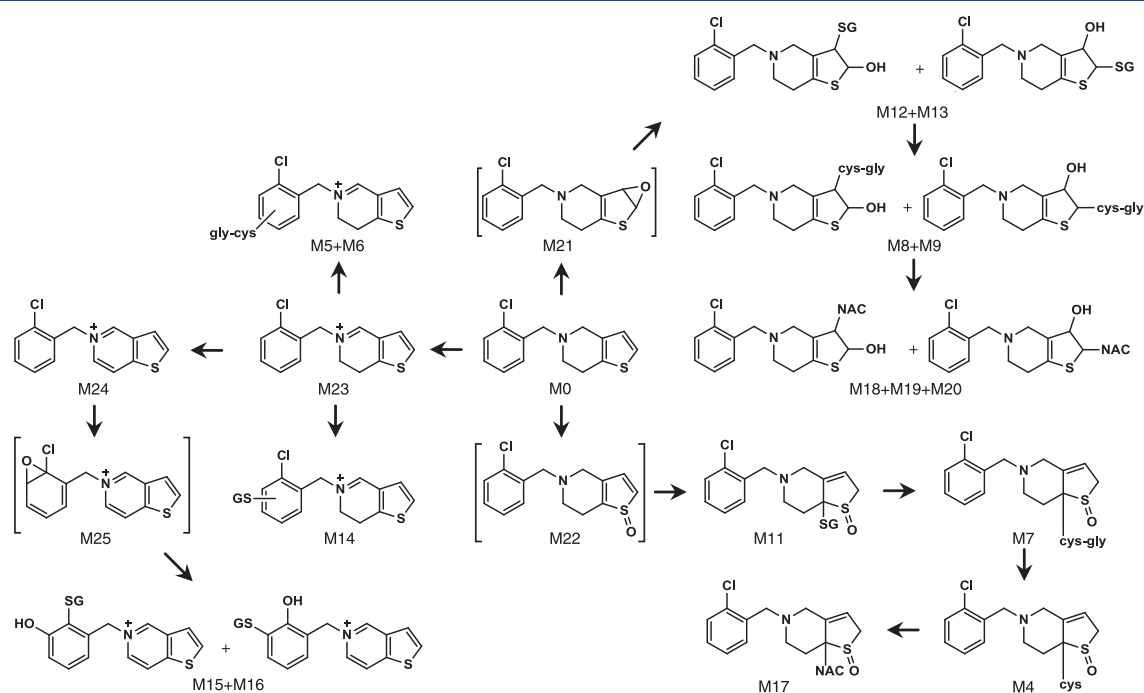
Figure 1. Proposed bioactivation pathway of ticlopidine in rats based on its conjugated metabolites found in rat bile from this study and the metabolism information reported in the literature. Definitive structures of ticlopidine metabolites (M23, M24 and M11) were previously determined using NMR (Refs. 6 and 7). Proposed structures of other metabolites were determined using HRMS.

chromatography (LC)-MS injections with different NL and PI scans are often required. Once unknown conjugated metabolites are detected by NL and/or PI scans, additional LC-MS experiments are performed to acquire their product ion (MS/MS) spectra for structural identification. Recently, high-resolution-MS (HRMS) has been increasingly used for drug metabolite detection and identification. In the HRMS experiments, full-scan MS and data-dependent MS/MS acquisition, such as intensity-, list- or isotope pattern-dependent methods, is performed to record both full-scan MS and MS/MS data in the same injections.[13,14] Then, post-acquisition data processes using mass defect filter (MDF),[15,16] extracted ion chromatogram (EIC) analysis, isotope pattern filter (IPF)[17,18] and other data-mining tools are carried out for fast and comprehensive searching of drug metabolites from full-scan MS and MS/MS dataset. The effectiveness of HRMS and post-acquisition data processing tools in identification of oxidative metabolites has been demonstrated in many examples in the literature.[13–15,18] However, there are limited reports of using HRMS for effective detection and structural characterization of drug conjugates in complex biological matrices. Conjugated drug metabolites have molecular weights significantly greater than oxidative metabolites. Effects of endogenous components and background noises in biological samples on the detection and identification of conjugated metabolites by HRMS are different from the detection of oxidative metabolites, which is dictated by similarities of molecular weights, mass defect values and isotope patterns of interference components to those of conjugated metabolites.[15] Therefore, analysis of drug conjugates using various types of HRMS data acquisition and processing techniques may not be as effective as analysis of oxidative metabolites.

The main objective of the current study was to develop an integral workflow for fast and comprehensive profiling and characterization of various classes of conjugated metabolites

using HRMS. The utility and limitation of various HRMS-based data acquisition and processing techniques in analyzing drug conjugates were evaluated. The secondary objective was to determine metabolic activation pathways of ticlopidine in rats. Results from analyzing biliary ticlopidine conjugates associated with reactive intermediates in rat bile, including glutathione (GSH), cysteinylglycine (cys–gly), cysteine (cys) and *N*-acetylcysteine (NAC) conjugates, provided insight into ticlopidine bioactivation in rats *in vivo*.

Experimental

Chemicals and reagents

Ticlopidine hydrochloride was purchased from Sigma-Aldrich (St. Louis, MO, USA). All other chemicals were purchased from Sigma-Aldrich or ThermoFisher Scientific (Waltham, MA). All compounds were of highest purity available.

Metabolism of ticlopidine in rats

Male Wistar rats (200–230 g) were supplied by Lab Animal Center of Shandong University (Grade II, Certificate No. SYXK 2003–0004). The experimental protocol was approved by the Shandong University Ethics Committee and conformed to the 'Principles of Laboratory Animal Care' (NIH Publication No. 85–23, revised 1985). Rats were fasted for 12 h before drug administration and for a further 3 h after dosing. Water was freely available for rats during experiments. Rats (*n* = 6) were given a single oral dose of ticlopidine hydrochloride (20 mg/kg) dissolved in distilled water. Bile samples were collected from 0 to 8 h after oral administration of ticlopidine, and 0.1% formic acid was added (1:1, v/v) in part of bile samples to stabilize the potential glucuronide conjugates.

Untreated and stabilized bile samples (0.5 ml) were filtered through a 0.22 μm micropore filter and then loaded onto pretreated solid-phase extraction cartridges (Oasis extraction cartridges, Waters Corp., Milford, MA). The cartridges were washed with 1 ml of water and then eluted with 1 ml of methanol. The methanol fractions were dried and reconstituted with 100 μl of initial mobile phase. Aliquots (20 μl) of the reconstituted solutions were injected onto LC-HRMS.

LC-MS conditions

All LC-MS experiments were carried out on a ThermoFisher Scientific LTQ/Orbitrap XL hybrid mass spectrometer equipped with an electrospray ionization interface. An Accela HPLC system (ThermoFisher Scientific) was equipped with an autosampler, a vacuum degasser unit and a quaternary pump. The mass spectrometer employing positive ionization was calibrated using the manufacturer's calibration standards mixture allowing for mass accuracies <5 ppm in external calibration mode. The ionization voltage was 4.2 kV, and the capillary temperature was set at 300°C. Nitrogen was used as both the sheath gas (40 units) and auxiliary gas (10 units).

A nominal mass difference of 2 Da and the ratio (0.32) of the nominal m/z corresponding to the isotopic doublet from full-scan mass analysis was used to trigger data-dependent MS/MS acquisition of ticlopidine metabolites. The resolving power was 15 000 for full scan and 7500 for the MS^2 scans. The $[M + H]^+$ PIs of ticlopidine and its metabolites were dissociated in the collision-induced dissociation (CID) or high collision energy dissociation (HCD) mode using the normalized collision energy at 35% with an isolation width of 3 Da and an activation time of 30 ms.

Chromatographic separation was achieved on a Zorbax SB C18 column (150 mm × 2.1 mm i.d., 5 μm; Agilent, Santa Clara, CA) with a 4.0 mm × 3.0 mm i.d. SecurityGuard C18 (5 μm) guard column (Phenomenex, Torrance, CA). The reversed-phase gradient LC-HRMS experiments were performed using a mobile phase A of 0.02% trifluoroacetic acid in H$_2$O and a mobile phase B of acetonitrile at a flow rate of 0.3 ml/min. The HPLC gradient system for metabolites characterization started with 15% B and linearly increased to 90% B in 20 min, followed by a decrease to 15% B in 2 min prior to column re-equilibration.

For online H/D exchange LC-MS experiments, deuterated water was used as the mobile phase A, i.e. deuterium oxide (D$_2$O) (100% atom D, ThermoFisher Scientific) with 0.02% D-trifluoroacetic acid (98% atom D, Sigma-Aldrich). Acetonitrile was used as the mobile phase B.

MS data processing

High-resolution MS data processing was carried out using the QualBrowser of Xcalibur 2.1 (Thermo Fisher Scientific), including EIC, calculation of elemental compositions using potential metabolite ions with 5-ppm mass tolerance and isotope pattern simulation. Multiple MDFs were carried out using MetWorks 1.3 (Thermo Fisher Scientific). On the basis of the structure of ticlopidine, the following MDF templates were applied to detect ticlopidine conjugates: (1) the glucuronide of monohydroxylated ticlopidine (m/z 456.088) and the NAC conjugate of ticlopidine (m/z 427.091); (2) the GSH adduct of ticlopidine (m/z 569.129); and (3) combination of (1) and (2). Specifically, the MDF windows were set to ± 0.060 Da around the mass defects of the templates over a mass range of ± 50 Da of the filter templates. Finally,

individual peaks present in MDF-processed ion chromatograms were subjected to a quick confirmation based on the accurate full-scan MS spectra. HR-IPF process was carried out using MsXelerator (MsMetrix, Maarssen, Netherlands). The windows of mass difference and intensity ratio for $^{35}Cl/^{37}Cl$ were set at 1.997 ± 5 ppm and 3 ± 1, respectively. Structures of the detected metabolites were characterized based on their MS shifts from the parent drug, fragmentation patterns and elemental compositions. In addition, Mass Frontier 6.0 (Thermo Fisher Scientific) was used in aiding MS/MS spectral interpretation of metabolites.

Results and discussion

Analytical strategy

An integrated strategy using various HRMS-based data acquisition and processing tools was applied to the detection and structural characterization of ticlopidine conjugates in rat bile. Accurate full-scan MS and MS/MS data were obtained mainly using an isotopic pattern triggered data-dependent MS/MS acquisition method. Both CID and HCD spectra were acquired at the same time. To search for both common and uncommon conjugated metabolites from recorded full-scan MS dataset, data mining techniques including EIC, IPF and MDF were performed at selected m/z ranges corresponding to various classes of drug conjugates. When a ticlopidine metabolite with the chlorine atom was found by any of these data processing techniques, its product ion spectrum was acquired in isotope-dependent product ion scanning analysis. Furthermore, an online H/D exchange experiment was carried out to confirm the exchangeable hydrogen atoms in metabolites for structural characterization. The strategy is also applicable to characterization of drug conjugates that have no distinct isotope patterns. In this case, intensity-, list- and/or mass defect-dependent acquisition method(s) can be employed to record MS/MS spectra of conjugated metabolites. It should be mentioned that this analytical strategy is also useful for profiling and characterization of oxidative metabolites, in which data processing is carried out in m/z ranges similar to and significantly smaller than the parent drugs.

Detection of conjugates of ticlopidine in rat bile

The total ion chromatogram (TIC) of the full-scan MS dataset revealed eight ticlopidine conjugates, some of which overlapped with endogenous components, while low abundant metabolites were buried in high levels of matrixes (Fig. 2A). IPF was able to selectively detect 18 ticlopidine conjugates with few false positive peaks based on their unique isotope pattern (Fig. 2B). However, the dechlorinated metabolites, M15 and M16 (P + O-4H-HCl + GSH), were not detected by IPF. Extracted ion chromatogram (EIC) was utilized to detect conjugated metabolites based on m/z values predicted from common biotransformation reactions or reported in the literature. As a result, 11 conjugates of ticlopidine including some metabolites with relatively low abundance were detected by EIC (Table 1). For example, M13 (P + O + GSH) and M16 (P + O − 4H − HCl + GSH) were clearly displayed in the profiles processed with EIC (Fig. 2C and 2D), but not visible in TIC (Fig. 2A).

Various MDF templates were utilized to detect ticlopidine conjugates in this study. The chemical background noise and matrix noise were significantly reduced after using the drug-related MDF filter templates. As a result, multiple glucuronide,
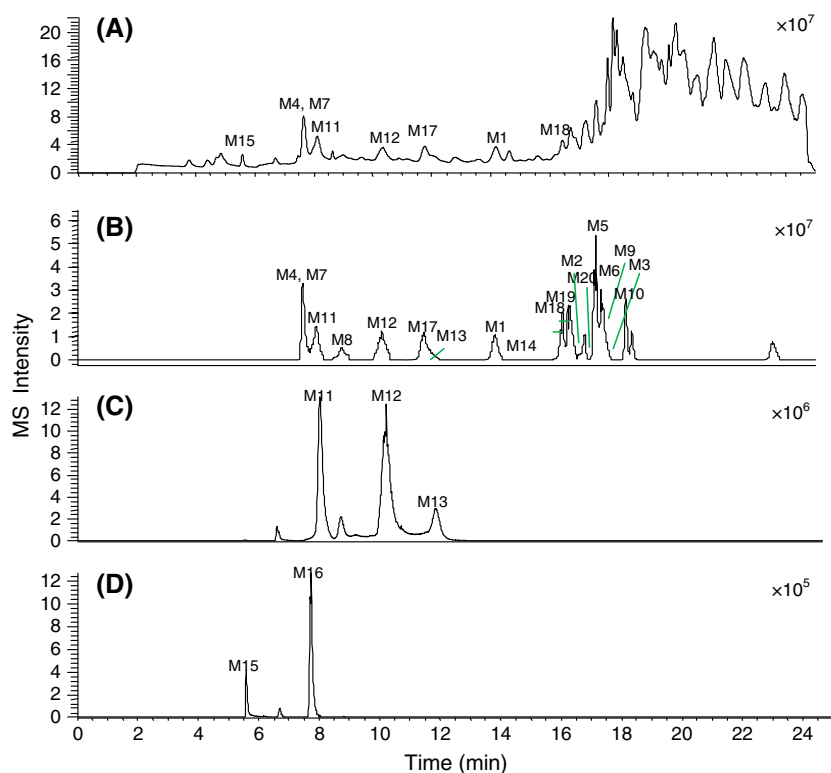
Figure 2. Metabolite profiles of ticlopidine in rat bile. (A) Unprocessed total ion chromatogram (TIC) (*m/z* 200–800), (B) Isotope pattern filter (IPF) processed profile (*m/z* 350–800), (C) Extracted ion chromatograms (EIC) of an ion at *m/z* 587.1395 (P + O + GSH) and (D) EIC of an ion at *m/z* 547.1316 (P + O-4H-HCl + GSH).

Table 1. Ticlopidine conjugates detected and characterized in rat bile by Orbitrap and multiple data mining tools

Metabolites	t_R (min)	*m/z* $[M+H]^+$	*m/z* $[M+D]^+$	Assignment	Major fragments obtained using CID mode (except for the data in the parentheses obtained using HCD mode)	IPF	MDF	EIC
M0	21.61	264.0616	265.0675	P (parent drug)	154, [a]125			
M1	14.19	456.0891	461.1203	P + O + Glu	[a]280, 154, 125	+	+	+
M2	16.84	456.0889	461.1204	P + O + Glu	280, [a]262, 154, 125	+	−	+
M3	17.91	488.1154	493.1465	P + O + CH$_2$ + H$_2$O + Glu	470, 442, 424, [a]312, 264, 154	+	+	−
M4	7.65	401.0766	405.1017	P + O + cys	383, [a]353, 280, 232, 154, 125	+	+	−
M5	17.56	440.0875	444.1128	P-2H + cys–gly	n.a.	+	+	−
M6	17.83	440.0876	444.1128	P-2H + cys–gly	n.a.	+	+	−
M7	7.68	458.0982	463.1296	P + O + cys–gly	440, [a]410, 305, 287, 280, 232, 154, 125	+	+	−
M8	9.00	458.0983	464.1357	P + O + cys–gly	[a]440, 305, 287, 280, 154	+	+	−
M9	17.79	458.0983	n.a.	P + O + cys–gly	[a]440, 305, 287, 280, 154	+	−	−
M10	18.61	454.0666	458.0918	P + O-4H + cys–gly	n.a.	+	+	−
M11	8.13	587.1413	594.1853	P + O + GSH	569, 539, 512, [a]458, 440, 410, 308, 296, 274, 232 (154, 125)	+	+	+
M12	10.37	587.1415	595.1914	P + O + GSH	569, 551, 494, [a]458, 440, 308, 287, (184, 154, 125)	+	+	+
M13	12.01	587.1415	595.1913	P + O + GSH	[a]569, 494, 458, 440, 308, 280, 264, (184, 154, 125)	+	+	+
M14	14.60	567.1151	573.1512	P-4H + GSH	550, 522, 510, 438, [a]294, 260, (136, 125)	+	+	−
M15	5.59	547.1329	n.a.	P + O-4H-HCl + GSH	472, 418, 337, 283, [a]274, 266, 180, (163, 139)	−	+	+
M16	7.72	547.1326	n.a.	P + O-4H-HCl + GSH	472, 418, 337, 283, [a]274, 266, 180, (163, 139)	−	+	+
M17	11.75	443.0873	446.1062	P + O + NAC	425, [a]395, 314, 296, 280, 232, 154, 125	+	+	+
M18	16.40	443.0875	447.1120	P + O + NAC	425, 314, 296, [a]280, 262, 232, 170, 154, 136, 125	+	+	+
M19	16.70	443.0874	447.1121	P + O + NAC	[a]425, 415, 314, 296, 280, 272, 230, 184, 154, 125	+	+	+
M20	17.22	443.0873	447.1120	P + O + NAC	425, 415, 314, 296, 280, 272, 230, 184, [a]154, 125	+	+	+
				Number of detected metabolites by each data mining method		18	18	11

n.a., not acquired;
[a], base peak in MS/MS spectrum.

N-acetylacysteine (NAC), cys–gly, and cys conjugates were detected using a combination of ticlopidine-glucuronide and NAC conjugate as a MDF template (Fig. 3A). In addition, six GSH conjugates were detected using ticlopidine-GSH as a MDF template (Fig. 3B). The combination of both MDFs was able to detect all of the 18 metabolites (Fig. 3C). MDF was capable of finding uncommon metabolites such as M3, a glucuronide (P + O + CH_2 + H_2O + Glu), from multiple steps of biotransformation. However, two minor metabolites, M2 and M9, were not found by MDF due to their low abundance. In addition, a few more false positives were generated as compared to IPF (Fig. 2B) and EIC (Fig. 2C and Fig. 2D). Conjugated metabolites of ticlopidine detected in rat bile using various data processing tools are summarized in Table 1.

Structural characterization of ticlopidine conjugates

M0

Unchanged ticlopidine ($C_{14}H_{15}NSCl$) eluted at 21.6 min and gave a protonated molecule ([M + H]$^+$) at *m/z* 264.061 (^{35}Cl) and 266.058 (^{37}Cl). The MS/MS spectrum of the ion at *m/z* 264 mainly displayed fragment ions at *m/z* 154.042 (C_8H_9NCl) and 125.015 (C_7H_6Cl), which related to charged chlorophenyl group in ticlopidine. The H/D exchange MS spectra of ticlopidine gave a protonated molecule at *m/z* 265.067 with an elemental composition of $C_{14}H_{14}DNClS$ ([M + D]$^+$), indicating ticlopidine has no exchangeable hydrogen atom.

M1 and M2

These two metabolites were detected at 14.2 min and 16.8 min, respectively, with the theoretical molecular ions at *m/z* 456.088 (P + O + Glu; $C_{20}H_{23}NSClO_7$). The protonated molecules displayed a characteristic product ion at *m/z* 280.056 ($C_{14}H_{15}NSClO$) by loss of the glucuronic acid (Fig. 4). Another two fragment ions at *m/z* 154.042 (C_8H_9NCl) and 125.015(C_7H_6Cl) indicated that

the oxygen atom was located on the tetrahydrothienopyridine moiety. As shown in Fig. 4A, the hydroxyl group in M1 could probably locate on the thiophene ring since it was relatively stable. The hydroxyl group in M2 was not stable, and the ion at *m/z* 262.045 ($C_{14}H_{13}NClS$; loss of one water molecule from P + O) was observed (Fig. 4B), which suggested that the hydroxylation probably happened on the tetrahydropyridine ring. The H/D exchange MS spectra of M1 and M2 showed five exchangeable hydrogen atoms: four from the glucuronic acid moiety and one from the charge.

M3

M3 was detected at 17.9 min with the theoretical protonated molecule at *m/z* 488.114 (P + O + CH_2 + H_2O + Glu; $C_{21}H_{27}NSClO_8$). The protonated molecules mainly displayed a product ion at *m/z* 312.082 ($C_{15}H_{19}NSClO_2$) by loss of the glucuronic acid (Fig. 4C). Two characteristic fragment ions at *m/z* 442.126 ($C_{20}H_{25}NClO_8$; loss of the methylthio group) and *m/z* 424.116 ($C_{20}H_{23}NClO_7$; loss of the methylthio group and one water molecule) were generated, which implied that M3 was a thiophene ring-opened metabolite and a methyl group was attached to the sulfur atom. It has been found that the *S*-oxide or epoxide intermediate could undergo a rearrangement to 2-oxo-ticlopidine, which was then biotransformed via thiophene ring opening into a pharmacologically active metabolite.[19,20] A carboxylic acid group was formed via this pathway. The product ion at *m/z* 264.078 ($C_{14}H_{15}NClO_2$) was generated by loss of the methylthio group and the glucuronic acid. In the H/D exchange MS spectra, no exchangeable proton was found for the aglycone moiety. All the data above indicated that M3 was an acylglucuronide of the thiophene ring-opened metabolite and the S-CH_3 group existed in its structure (Fig. 4C).

M4

The metabolite M4 was determined at *m/z* 401.076 (P + O + Cys; $C_{17}H_{22}N_2S_2ClO_3$). The characteristic NL of cys (121.019 Da)
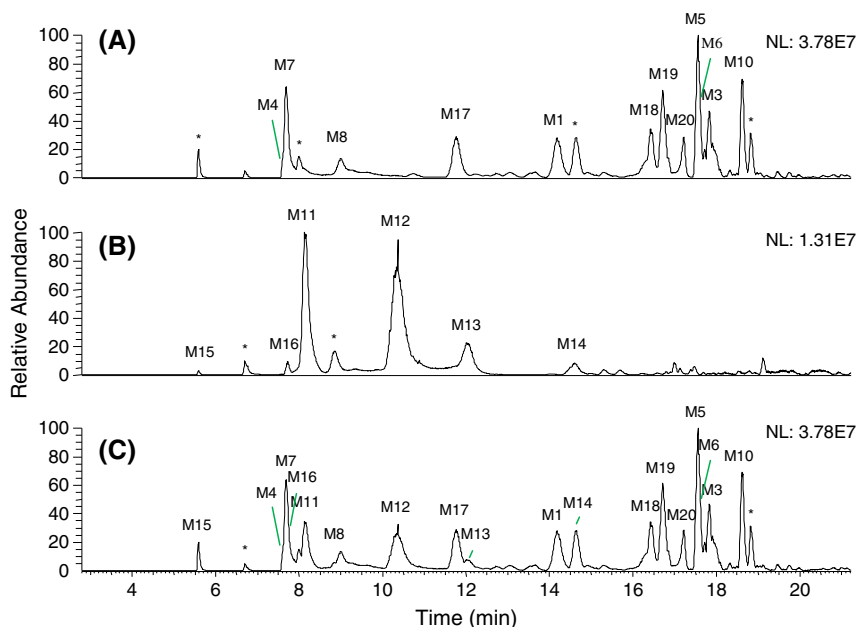
Figure 3. High-resolution mass defect filter (MDF) chromatograms for ticlopidine conjugates in rat bile. (A) MDF of Glu and NAC conjugates; (B) MDF of GSH adducts; (C) combined MDF of Glu, NAC and GSH conjugates (*, false positives).
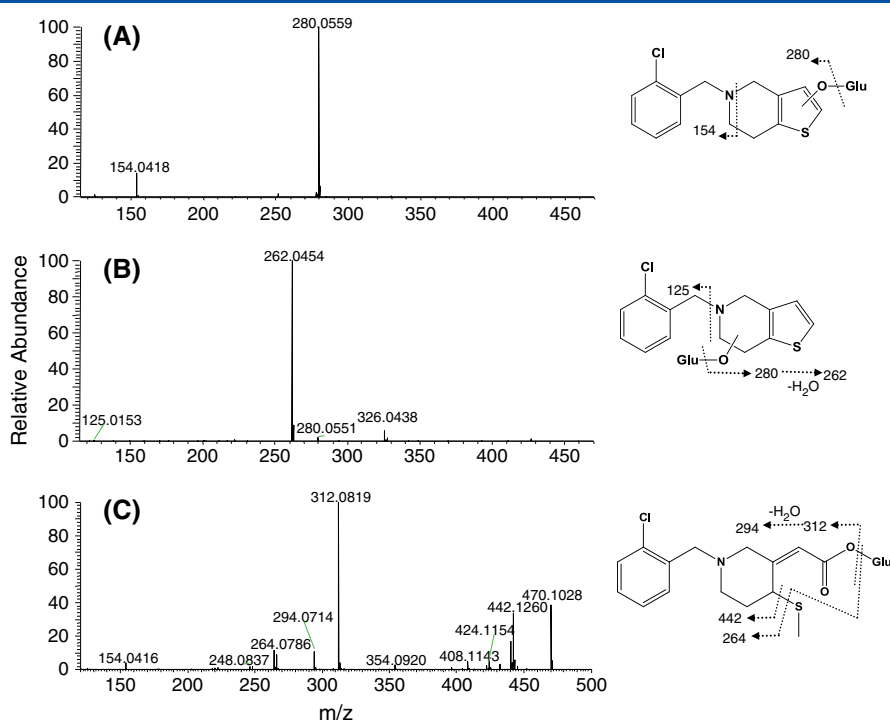
Figure 4. MS/MS spectra and proposed structures of ticlopidine glucuronides M1 (A), M2 (B) and M3 (C) detected in rat bile.
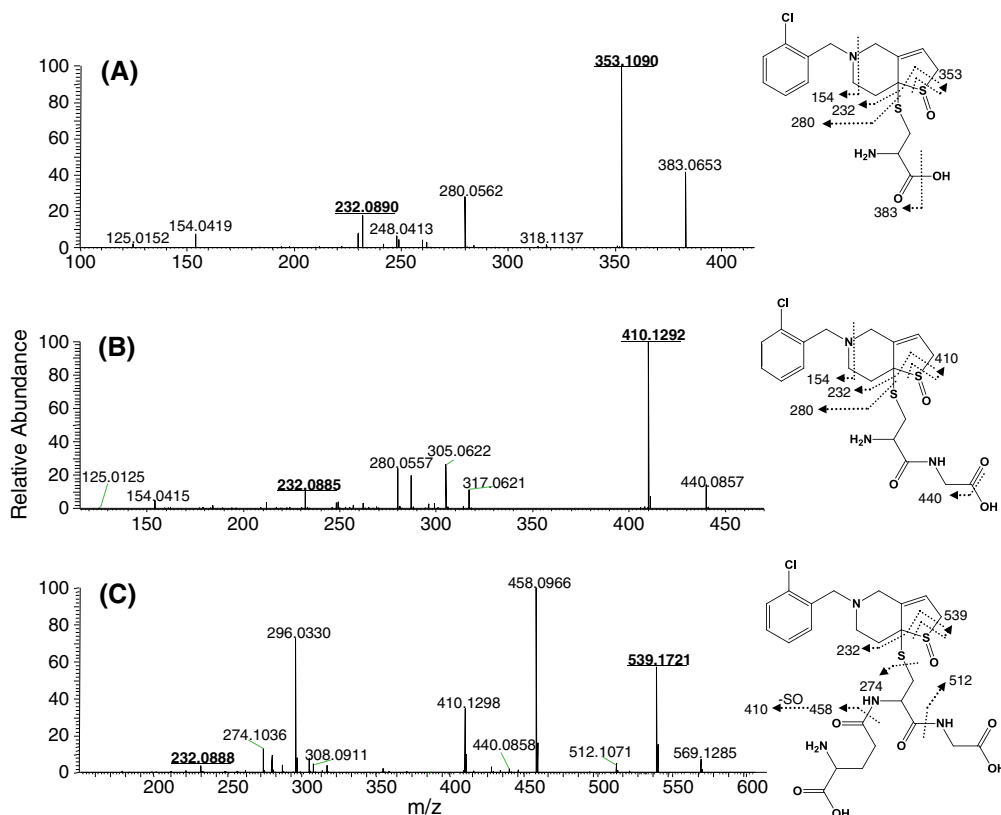
Figure 5. MS/MS spectra and proposed structures of thiophene-S-oxide conjugates of ticlopidine in rat bile: (A) M4, (P + O + cys, *m/z* 401.076); (B) M7, (P + O + cys–gly, *m/z* 458.097) and (C) M11, (P + O + GSH, *m/z* 587.141).

resulted in the product ion at *m/z* 280.056 (C₁₄H₁₅NSClO) (Fig. 5A). NL of the sulfoxide (47.969 Da) group and subsequent loss of cys generated fragments at *m/z* 353.109 and *m/z* 232.089,

respectively, indicating the presence of a sulfoxide moiety. Thus, M4 was proposed to be the cys conjugate of thiophene-S-oxide reactive intermediate (Fig. 5A).

M5 and M6

These two metabolites with the same protonated molecule were detected at 17.6 min and 17.8 min, respectively. Unfortunately, their MS/MS spectra were not acquired during data-dependent acquisition due to their low abundance. M5 was determined at m/z 440.087 in the full-scan spectrum (Fig. S1), which was 2.5 ppm different from the theoretical value of the protonated cys–gly conjugates of the dihydropyridinium metabolite, (P-2H + cys–gly; $C_{19}H_{23}N_3S_2ClO_3$). Moreover, determined isotopic peaks of the protonated molecule and their relative intensities matched those of $C_{19}H_{23}N_3S_2ClO_3$, which was simulated using QualBrowser (resolution < 5 ppm, and isotopic ratios < 20%) (Fig. S1). Thus, M5 and M6 were identified as cys–gly conjugates of ticlopidine. Most likely, M5 and M6 were derived from ticlopidine GSH adducts that were formed via a chlorophenyl epoxide intermediate (Fig. 1). The same cys–gly conjugates of ticlopidine were previously observed in liver microsomal incubations.[21]

M7–M9

These metabolites with the same protonated molecule at m/z 458.097 (P + O + cys–gly; $C_{19}H_{25}N_3S_2ClO_4$) were detected at 7.7 min, 9.0 min and 17.8 min. They shared the product ion at m/z 280.056 ($C_{14}H_{15}NSClO$, P + O) derived from a characteristic NL of cys–gly ($C_5H_{10}N_2SO_3$; 178.041). A NL of 47.969 Da from the parent ion leading to a product ion at m/z 410.129 was observed in the MS/MS spectrum of M7, indicating that M7 was a cys–gly conjugate originated from thiophene-S-oxide reactive intermediate (Fig. 5B). M8 and M9 displayed multiple ions (Table 1), all of which were observed in the MS/MS spectra of M7 except for the ion at m/z 410.128. The data implied that M8 and M9 were cys–gly conjugates of hydroxylated ticlopidine and formed from GSH adducts of a thiophene epoxide. The proposed structures and formation pathways of M8 and M9 are shown in Fig. 1.

M10

This metabolite eluted at 18.6 min displayed the protonated molecule at m/z 454.067 in the full-scan spectrum, which was 2.1 ppm different from the theoretical m/z value of the protonated molecule with chemical composition of P + O-4H + cys–gly. In addition, the measured isotopic peaks of M10 matched with the corresponding isotope peaks of the $C_{19}H_{21}N_3S_2ClO_4$ molecule that was simulated using QualBrowser. Based on the mass spectral data, M10 was proposed as a cys–gly conjugate of the dihydrothienopyridinium metabolite of monooxidized ticlopidine (Table 1).

M11–M13

The [M + H]$^+$ ions of M11–M13 were determined at m/z 587.139 (P + O + GSH; $C_{24}H_{32}N_4S_2ClO_7$). The characteristic NL of glycine (75.029), pyroglutamate (129.044) and GSH (307.083) from the GSH moiety led to the product ions at m/z 512.107 ($C_{22}H_{27}N_3S_2ClO_5$), m/z 458.097 ($C_{19}H_{25}N_3S_2ClO_4$) and m/z 280.056 ($C_{14}H_{15}NSClO$), respectively. A NL of 47.969 Da from the protonated molecule of M11 (m/z 539.172) (Fig. 5C) indicated that this GSH adduct was originated from the thiophene-S-oxide reactive intermediate (M22, Fig. 1). In the deuterium exchange spectra of M11, seven protons of the protonated GSH adduct were subjected to substitution by deuterium: six from the GSH and one from the positive charge. The observation confirmed that the oxygen was attached to the S atom. The same GSH adduct was observed in rat liver microsomal incubations[4] and rat bile.[7] M12 and M13

showed diagnostic ions at m/z 154.042 (C_8H_9NCl) and m/z 125.015 (C_7H_6Cl), which indicated that oxidation occurred on the tetrahydrothienopyridine moiety. Eight exchangeable hydrogen atoms found in the H/D exchange spectra of M12 and M13 suggested the addition of a hydroxyl group. Proposed structures and formation pathways of M12 and M13 are displayed in Fig 1. M12 and M13 were a pair of positional isomers that were formed via addition of a GSH to a thiophene epoxide intermediate (M21). A GSH adduct of the thiophene epoxide intermediate was previously observed in rat liver microsomal incubations.[4]

M14

The protonated molecule of M14 was determined at m/z 567.113 (P + GSH-4H; $C_{24}H_{28}N_4S_2ClO_6$), which suggested that M14 was formed via ticlopidine dehydrogenation followed by GSH addition. CID and HCD spectra of M14 are shown in Fig. 6. Characteristic NLs of pyroglutamate (129.044) and GSH (307.083) led to product ions at m/z 438.075 ($C_{19}H_{21}N_3S_2ClO_3$) and m/z 260.030 ($C_{14}H_{11}NSCl$), respectively, which confirmed that it was a GSH adduct. Interestingly, the CID spectrum exhibited multiple, large fragment ions from the GSH moiety, but no intense small product ions associated with the drug moiety (Fig. 6A). In contrast, the HCD spectrum of M14 displayed a few smaller fragment ions without large fragments observed in the CID spectrum (Fig. 6B). The product ion at m/z 125.0152 provided a key evidence for the presence of the ticlopidine moiety in the GSH conjugate (Fig. 6B). The results suggested that a combination of CID and HCD provides both small and large fragments for GSH adducts, which is useful for their structure characterization. M14 was proposed as a GSH conjugate of the dihydrothienopyridinium metabolite of ticlopidine (M23). It was reported that M23 is a major metabolite formed in HLM.[22] Most likely, M23 underwent epoxidation on the chlorophenyl moiety, followed by addition of GSH and loss of a water molecule, resulting in M14 (Fig. 1).
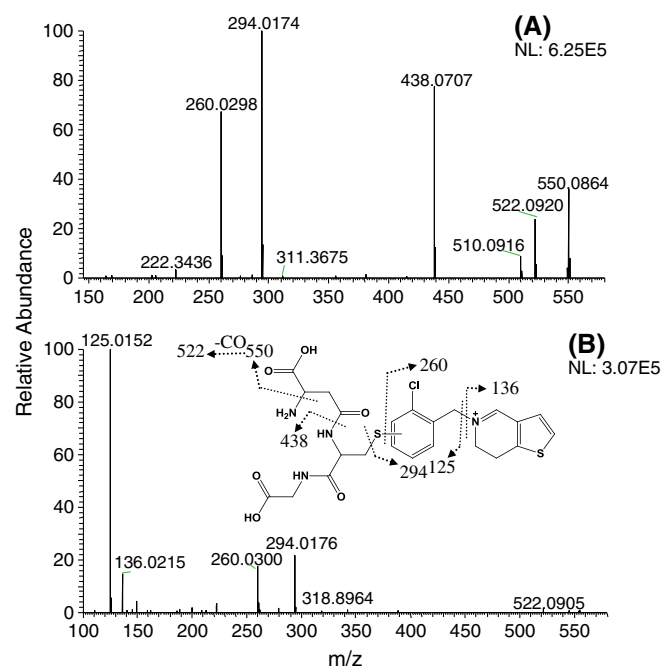

Figure 6. MS/MS spectra of M14 obtained by (A) collision-induced dissociation (CID) and (B) high collision energy dissociation (HCD). The proposed structure of M14 is shown in Figure 4B.

M15 and M16

The $[M+H]^+$ ions of M15 and M16 were found at *m/z* 547.132 (P + O-4H-HCl + GSH; $C_{24}H_{27}N_4S_2O_7$). The characteristic NL of glycine (75.029) and pyroglutamate (129.044) led to the product ions at *m/z* 472.099 ($C_{22}H_{22}N_3S_2O_5$) and *m/z* 418.089 ($C_{19}H_{20}N_3S_2O_4$), respectively, suggesting that these are GSH adducts. The lack of intense M + 2 isotope ions in the full-scan MS spectra of M15 (Fig. S2) and M16 indicated the loss of the chlorine atom in their structures. The fragment ions at *m/z* 337.085 and *m/z* 283.075 suggested the dehydrogenation of the tetrahydrothienopyridine moiety (loss of 4H) and the GSH conjugation to the phenyl moiety. It is thus proposed that the epoxidation took place on the chlorophenyl moiety, followed by epoxide ring opening accompanying nucleophilic addition of GSH and dechlorination. The product ion at *m/z* 274.036 ($C_{14}H_{12}NS_2O$) was derived from the cleavage of C–S bond of the GSH moiety, and subsequent fragment ions at *m/z* 180.048 ($C_9H_{10}NSO$), 163.021 (C_9H_7SO) and 139.021 (C_7H_7SO) were also observed (Fig. S2).

M17–M20

These four metabolites had the same protonated molecule at *m/z* 443.086 (P + O + NAC; $C_{19}H_{24}N_2S_2ClO_4$), and a product ion at *m/z* 280.056 raised from the loss of an NAC moiety, which suggested that M17–M20 were NAC conjugates of ticlopidine mono-oxidation products. The deuterium exchange spectrum of M17 showed three exchangeable protons: two from the NAC and one from the positive charge (Fig. 7). The product ions at *m/z* 395.118 ($C_{19}H_{24}N_2SClO_3$) for M17 by loss of SO suggested that this metabolite was the NAC conjugate of thiophene-*S*-oxide, which has also been observed in another study.[7] Four exchangeable hydrogen atoms were found in the H/D exchange spectra of M18–M20, which suggested that a hydroxyl group existed in their structures. Metabolites M18–M20 showed product ions at *m/z* 154.042 and *m/z* 125.015, which indicated that the oxygen was located on the tetrahydrothienopyridine moiety.
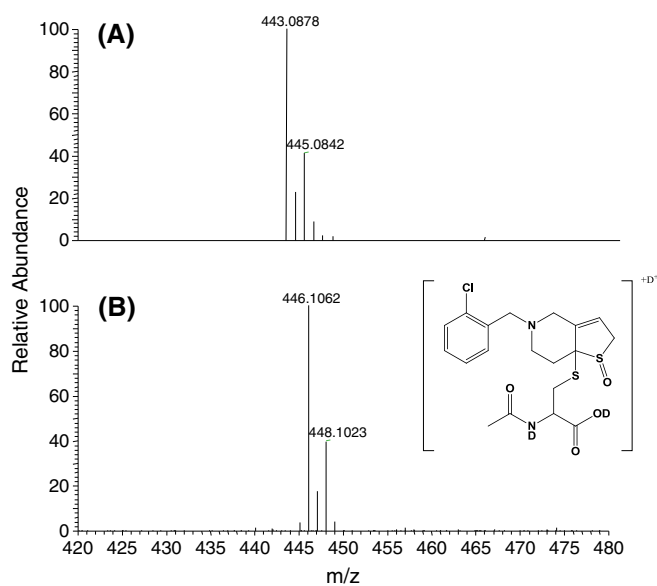
Comparison of various data acquisition and processing tools

In the present study, an analytical strategy using various data acquisition methods were applied to the detection and characterization of ticlopidine conjugates. Isotope pattern-triggered data-dependent acquisition was able to selectively record accurate full-scan MS data of all PIs as well as MS/MS data of most ticlopidine conjugates based on the isotope pattern of chorine-containing structures (Table 1). For compounds that have a distinct isotope pattern at a known percentage, either due to the presence of natural isotopes (Cl, Br, etc.) or stable-labeled isotope analogues (^2H, ^{13}C, ^{15}N, etc.), this dependent MS/MS acquisition has always been a favorable choice. In contrast to NL and PI scan, isotopic pattern-triggered MS/MS scan does not rely on fragmentation patterns and thus is selective and sensitive in the data acquisition of metabolites that have unique isotope pattern. For data acquisition of conjugated metabolites derived from drugs that have no unique isotope patterns, other data-dependent MS/MS acquisition methods can be applied, which include list-, intensity- and mass defect-triggered MS/MS acquisition. In addition to CID spectra, HCD spectra of ticlopidine conjugates were recorded using the same data-dependent method. HCD produced more small and less large fragments than CID. The combination of CID and HCD provided rich and comprehensive fragments for conjugated metabolites, which is especially useful for structural characterization of conjugates that usually display a few large fragments via CID. The utility of the combination of CID and HCD has been demonstrated in characterization of several conjugated metabolites of ticlopidine such as M14 (Fig. 6). Furthermore, the current strategy included a step to acquire PI spectra of ticlopidine conjugates after H/D exchanging, which allowed distinguishing *N*- and *S*-oxide from mono-hydroxylated metabolites. For example, a key evidence for characterization of conjugates of ticlopidine *S*-oxide (M4, M7, M11 and M17) was from the H/D exchanging experiment (Fig. 7). Another good example was the structural characterization of M3, an acyl glucuronide conjugate, which did not have any exchangeable proton in the drug moiety (Fig. 4C).

Multiple data mining techniques, including MDF, IPF, EIC, NLF, PIF and/or background subtraction, have been extensively used to process either full-scan MS or MS/MS data for fast and effective detection of oxidative metabolites. In the current data processing strategy, a combination of IPF, EIC and MDF was employed for detection of conjugated metabolite ions. The task was accomplished by processing accurate mass full-scan MS dataset in selected *m/z* ranges of different classes of ticlopidine conjugates. As shown in IPF (Fig. 2B) and EIC (Fig. 2C and 2D) processed metabolite profiles of rat bile, both data mining techniques had good selectivity and sensitivity for detecting conjugated metabolites. Metabolites that have no chorine atom (M15 and M16) or not easily predicable molecular weights (M3–M10, M14) were not found by IPF or EIC, respectively. In contrast, MDF was able to recover most of conjugated metabolites from the full-scan MS dataset based on their predictable mass defects rather than their unique isotope pattern or predicable molecular weights (Fig. 3 and Table 1). The downside of MDF is its relatively poor selectivity, which resulted in more false positives. MDF profiles had relatively high background levels, which made it difficult to display minor metabolites, such as M2 and M9. The results from analysis of ticlopidine conjugates in rat bile indicated that each of the three data processing tools has its own advantages and limitations. Another useful application of high-resolution full-scan

Figure 7. Representative mass spectra of M17 before deuterium exchange (A) and after deuterium exchange (B). The proposed structure of M17 is shown in Fig. 7B.

MS data is the use of isotope simulation technique to increase confidence of molecular formula determination of minor conjugated metabolites that does not have MS/MS spectral data. For example, three cys–gly conjugates of ticlopidine (M5, M6 and M10) were identified in bile solely based on their protonated molecules and associated isotope patterns (Fig. S1). We highly recommend using multiple data processing tools to improve the selectivity, sensitivity and comprehensiveness of data mining in search for PIs of conjugated metabolites. It should be pointed out that the mass spectral data acquired for analysis of ticlopidine conjugates are useful for detection and characterization of oxidative metabolites of ticlopidine.

Bioactivation pathways of ticlopidine in rats

Metabolic activation of ticlopidine has been extensively studied *in vitro*. GSH trapping experiments showed that the formations of thiophene *S*-oxide (M22) and thiophene epoxide (M21) that lead to multiple GSH adducts are major bioactivation pathways in human and rat liver microsomes (Fig. 1). Ticlopidine forms much more GSH adducts in rat liver microsomes than in HLM.[4,23] In addition to the formation of thiophene *S*-oxide (M22) and epoxide (M21) intermediates of the parent drug, several other oxidative metabolites of ticlopidine, including mono-oxidation and *N*-dealkylation products, also undergo *S*-oxidation and epoxidation-mediated activation that lead to many minor GSH adducts in rat liver microsomes.[4] Radiolabeled metabolism and disposition study in rats showed that biliary excretion is the major elimination pathway of radioactivity in rats and GSH adducts derived from reactive intermediates, M21 and M22, are major drug related components in rat bile.[7] An NAC adduct derived from GSH adduct of ticlopidine *S*-oxide (M17) was also observed in rat. However, the radiolabeled study did not find additional GSH, NAC, cys and cys–gly adducts.

The current study employed an improved LC-MS approach that enabled the comprehensive and sensitive detection of various conjugated metabolites. As a result, 20 ticlopidine conjugates were structurally characterized in rat bile, 17 of which, including GSH, cys, cys–gly and NAC adducts, were derived from reactive intermediates (Table 1). Based on the findings and data reported in the literature, bioactivation pathways of ticlopidine in rats are proposed and illustrated in Fig. 1. The formation of thiophene *S*-oxide and epoxide intermediates (M22 and M21) were major bioactivation pathways of ticlopidine in rats. M22 and M21 were trapped by GSH to form major GSH adducts, M11, M12 and M13. Additional bioactivation pathways in rats are the formation of GSH adducts M15 and M16 via an epoxide intermediate of thienopyridium (M25). Thienopyridium (M24) was previously observed as a major metabolite in HLM.[22] The indirect observation of the formation of M22, M21 and M25 intermediates in rats is consistent with results from *in vitro* GSH trapping experiments.[4] Detection of a minor GSH adduct M14 suggests that an epoxide intermediate of dihydrothienopyridium was formed in rats (Fig. 1). It was reported that dihydrothienopyridium is a major metabolite formed in HLM.[22] However, the ticlopidine bioactivation pathway via dihydrothienopyridium, which led to M14 (Fig. 1), has not been reported in the literature. In addition, two minor cys–gly conjugates, M5 and M6, were detected in rat bile, which is consistent with a previous observation from *in vitro* GSH trapping experiment.[21] The major inconsistency of the *in vitro* GSH trapping experiments reported in the literature[4,23] and the current *in vivo* studies in rats were the observation of many GSH adducts (or their derivatives) from oxidative metabolites of ticlopidine in rat liver microsomes, but not in rat bile. Most likely, primary oxidative metabolites initially formed were accumulated and then catalyzed by CYPs to reactive intermediates during the incubation in rat liver microsomes. In contrast, the same primary oxidative metabolites formed in liver *in vivo* could be quickly eliminated via bile or urine directly or undergo glucuronidation to form glucuronides, such as M1, M2 and M3. Therefore, extensive oxidations of these primary oxidative metabolites did not occur in rats *in vivo*. The comparison of *in vitro* and *in vivo* bioactivation of ticlopidine in rats indicates that primary bioactivation pathways observed in GSH trapping experiments in rat liver microsomes are good prediction of bioactivation in rats *in vivo*.

Conclusions

In this study, an improved analytical strategy has been developed and tested for rapid detection and characterization of conjugated metabolites in complex biological matrix. In addition to accurate full-scan MS spectra, both CID and HCD spectra of conjugated metabolites were acquired via a data-dependent manner. Furthermore, mass spectral data from online H/D exchanging experiment was recorded to facilitate structural elucidation. Post-acquiring data mining to discover conjugated metabolites was accomplished using IPF, EIC and MDF, each of which employed a different mechanism for metabolite search, and processed data were complementary (Table 1). Results from this study suggest that HRMS-based data acquisition and processing techniques, which are mainly developed for analysis of oxidative metabolites, are also applicable to the detection and characterization of conjugated metabolites in biological matrices. Among 20 ticlopidine conjugates found in rat bile, 17 conjugates were either GSH adducts and their downstream metabolites, such as cys–gly, cys or NAC conjugates (Table 1), indicating bioactivation was major metabolic pathways of ticlopidine in rats. Ticlopidine *S*-oxide (M22), epoxide of thiophene (M21) or further metabolism products of dihydrothienopyridium (M23) mediated the formation of GSH adducts and derivatives of GSH adducts (Fig. 1). The bioactivation pathways of ticlopidine observed in rats were predicted by the data from reactive metabolite-trapping experiment in rat liver microsomes although the *in vitro* system generated much more GSH adducts.

Supporting information

Supporting information may be found in the online version of this article.

References

[1] A. K. Jacobson. Platelet ADP receptor antagonists: ticlopidine and clopidogrel. *Best Pract. Res. Clin. Haematol.* **2004**, *17*, 55.

[2] T. R. Whetsel, D. M. Bell. Rash in patients receiving ticlopidine after intracoronary stent placement. *Pharmacotherapy* **1999**, *19*, 228.

[3] S. Noble, K. L. Goa. Ticlopidine. A review of its pharmacology, clinical efficacy and tolerability in the prevention of cerebral ischaemia and stroke. *Drugs Aging* **1996**, *8*, 214.

[4] Q. Ruan, M. S. Zhu. Investigation of bioactivation of ticlopidine using linear ion trap/orbitrap mass spectrometry and an improved mass defect filtering technique. *Chem. Res. Toxicol.* **2010**, *23*, 909.

[5] J. J. Bruno, B. A. Molony. In *New Drugs Annual: Cardiovascular Drugs*, (Ed: A. Scriabine), Raven: New York, **1983**, 295–316.

[6] D. K. Dalvie, T. N. O'Connell. Characterization of novel dihydrothieno-pyridinium and thienopyridinium metabolites of ticlopidine in vitro: role of peroxidases, cytochromes p450, and monoamine oxidases. *Drug Metab. Dispos.* **2004**, *32*, 49.

[7] S. Shimizu, R. Atsumi, T. Nakazawa, Y. Fujimaki, K. Sudo, O. Okazaki. Metabolism of ticlopidine in rats: identification of the main biliary metabolite as a glutathione conjugate of ticlopidine S-oxide. *Drug Metab. Dispos.* **2009**, *37*, 1904.

[8] P. Valadon, P. M. Dansette, J. P. Girault, C. Amar, D. Mansuy. Thiophene sulfoxides as reactive metabolites: Formation upon microsomal oxidation of a 3-aroylthiophene and fate in the presence of nucleophiles in vitro and in vivo. *Chem. Res. Toxicol.* **1996**, *9*, 1403.

[9] P. M. Dansette, G. Bertho, D. Mansuy. First evidence that cytochrome P450 may catalyze both S-oxidation and epoxidation of thiophene derivatives. *Biochem. Biophys. Res. Commun.* **2005**, *338*, 450.

[10] N.-T. Ha-Duong, S. Dijols, A.-C. Macherey, J. A. Goldstein, P. M. Dansette, D. Mansuy. Ticlopidine as a selective mechanism-based inhibitor of human cytochrome P450 2C19. *Biochemistry* **2001**, *40*, 12112.

[11] A. Garg, B. Prasad, H. Takwani , M. Jain , R. Jain, S. Singh. Evidence of the formation of direct covalent adducts of primaquine, 2-tert-butylprimaquine (NP-96) and monohydroxy metabolite of NP-96 with glutathione and N-acetylcysteine. *J. Chromatogr. B* **2011**, *879*, 1.

[12] M. Giorgi, G. Mengozzi, A. Raffaelli, A. Saba. Characterization of in vivo plasma metabolites of tepoxalin in horses using LC-MS-MS. *J. Pharm. Biomed. Anal.* **2011**, *56*, 45.

[13] F. Y. Du, T. Liu, T. Liu, Y. M. Wang, Y. K. Wan, J. Xing. Metabolite identification of triptolide by data-dependent accurate mass spectrometric analysis in combination with online H/D exchange and multiple data mining techniques. *Rapid Commun. Mass Spectrom.* **2011**, *25*, 3167.

[14] H.-K. Lim, J. Chen, K. Cook, C. Sensenhauser, J. Silva, D. C. Evans. A generic method to detect electrophilic intermediates using isotopic pattern triggered data-dependent high-resolution accurate mass spectrometry. *Rapid Commum. Mass. Spectrom.* **2008**, *22*, 1295.

[15] H. Y. Zhang, D. L. Zhang, K. Ray, M. S. Zhu. Mass defect filter technique and its applications to drug metabolite identification by high-resolution mass spectrometry. *J. Mass Spectrom.* **2009**, *44*, 999.

[16] Y. Liang, G. J. Wang, L. Xie, L. S. Sheng. Recent development in liquid chromatography/mass spectrometry and emerging technologies for metabolite identification. *Curr. Drug Metab.* **2011**, *12*, 329.

[17] L. Ma, B. Wen, Q. Ruan, M. S. Zhu. Rapid screening of glutathione-trapped reactive metabolites by linear ion trap mass spectrometry with isotope pattern-dependent scanning and postacquisition data mining. *Chem. Res. Toxicol.* **2008**, *21*, 1477.

[18] F. Cuyckens, R. Hurkmans, J. M. Castro-Perez, L. Leclecq, R. J. Mortishire-Smith. Extracting metabolite ions out of a matrix background by combined mass defect, neutral loss and isotope filtration. *Rapid Commun. Mass Spectrom.* **2009**, *23*, 327.

[19] K. Yoneda, R. Iwamura, H. Kishi, Y. Mizukami, K. Mogami, S. Kobayashi. Identification of the active metabolite of ticlopidine from rat in vitro metabolites. *Br. J. Pharmacol.* **2004**, *142*, 551.

[20] N. A. Farid, A. Kurihara, S. A. Wrighton. Metabolism and disposition of the thienopyridine antiplatelet drugs ticlopidine, clopidogrel, and prasugrel in humans. *J. Clin. Pharmacol.* **2010**, *50*, 126.

[21] T. Rousu, O. Pelkonen, A. Tolonen. Rapid detection and characterization of reactive drug metabolites in vitro using several isotope-labeled trapping agents and ultra-performance liquid chromatography/time-of-flight mass spectrometry. *Rapid Commun. Mass Spectrom.* **2009**, *23*, 843.

[22] J. C. Talakad, M. B. Shah, G. S. Walker, C. Xiang, J. R. Halpert, D. Dalvie. Comparison of in vitro metabolism of ticlopidine by human cytochrome P450 2B6 and rabbit cytochrome P450 2B4. *Drug Metab. Dispos.* **2011**, *39*, 539.

[23] B. Wen, L. Ma, S. D. Nelson, M. S. Zhu. High-throughput screening and characterization of reactive metabolites using polarity switching of hybrid triple quadrupole linear ion trap mass spectrometry. *Anal. Chem.* **2008**, *80*, 1788.